Mechanisms Forcing the Diurnal Cycle of Dust in an Arid Closed Basin

Tyler W. Barbero*, Amato T. Evan, Trinity R. Robinson

Scripps Institution of Oceanography, University of California, San Diego, La Jolla, California

ABSTRACT

The Salton basin is an arid, sub-sea level basin located in southeastern California. Mountain ranges border the basin directly to the west and east, to the north extends a narrow valley that terminates with a transverse mountain range, and to the south spans heavily irrigated, agricultural lands that gradually rise in surface elevation. Within the basin lies the Salton Sea, and surrounding the Sea is diverse terrain that includes dry playa, rocky and vegetated surfaces, and highly emissive alluvial fans and dry washes, among others. Although large dust outbreaks due to orographically forced high wind speed events are frequent in the area, measurements from a new AERONET site stationed within the basin shows that dust is a standard component of the region's atmosphere, even on days with otherwise low wind speeds. We find a diurnal cycle of background dustiness that peaks in the early afternoon. An analysis of boundary layer structure using a Vaisala CL51 suggests that deepening of the boundary layer due to dry convection results in downward mixing of momentum, increased surface wind speeds, and an accumulation of dust in the mixed layer. Further analysis of the CL51 observations at nighttime suggest that high AOD concentrations persist in the shallow nocturnal boundary layer, and can become elevated throughout the night due to westerly katabatic flows. An analysis of surface meteorological station data suggests possible pathways of suspended dust due to mountain and valley flows within the basin.

1. Introduction

The Salton Basin is located in southeastern California. This region is characterized by a hot, arid desert climate, receiving less than 100mm of precipitation per year. Temperature ranges on average from 12°-15°C during the winter and often exceeds 40°C in the summer (Ives 1949). Lying in the Basin's center at 72 meters below sea level is the Salton Sea. The Salton Sea is a shallow, endorheic rift lake due to the nature of how it was formed. Ramifications of its creation are such that the Sea's salinity and surface level fluctuate dynamically with trends revealing an acceleration of the shrinking of its surface area and an increase in water salinity (Forsman 2014). This suggests the Salton Basin will become more arid over time. Surrounding the Salton Sea, morphology includes but is not limited by rocky and vegetated surfaces, playa, dry washes, alluvial fans, and sand dunes.

Regional climate and terrain provide the area with a quintessential source of material for dust emission. This material is mainly dry, loose soil that can be lifted by the wind into the atmosphere as dust. There are a couple different weather phenomenon that cause dust emission. Outflow boundaries, otherwise known as gust fronts, are the result of divergent cooled air from the downdrafts of thunderstorms. Dust can be knocked up by the outflow boundary and carried along with it in an intense type of dust storm called a haboob. Haboobs are native to arid regions around the world such as the Saharan Desert and central Australia. Another process of dust emission is caused by orographically forced high wind speed events, called downslope windstorms. These events occur in the lee of the mountain when high altitude air descends down the mountain face and under appropriate conditions, high speed winds can reach the bottom and be able to knock dust into the atmosphere. As a result of prior research, downslope windstorms were found to be the main method of dust emission in the Salton Basin (Evan 2019). Additionally, observations from a new research site within the Salton Basin reveal peaks in aerosols coincident with these dust storms. However, observations also suggest that dust is a regular component of the region's atmosphere, even on days with otherwise low wind speeds. Here, we differentiate dust emission caused by background forcing from dust caused by downslope windstorms as background dust. Through an analysis of AERONET data, we find a moderate concentration of background dust that is consistent throughout the day and slightly peaks in the afternoon. We suspect that dust concentrations are forced by a combination of dry convection leading to a downward mixing of momentum and increase in surface wind speed, and thermally driven flows.

In this paper, we present a conceptual model for the mechanisms forcing the background diurnal cycle of dust within the Salton Basin. The remainder of the paper goes as follows: in Section 2, I give a broad overview of the types of observations used in various analyses. In section 3, I discuss the mechanisms forcing background dust on 29 February

*Corresponding author: Tyler Barbero, tbarbero@ucsd.edu

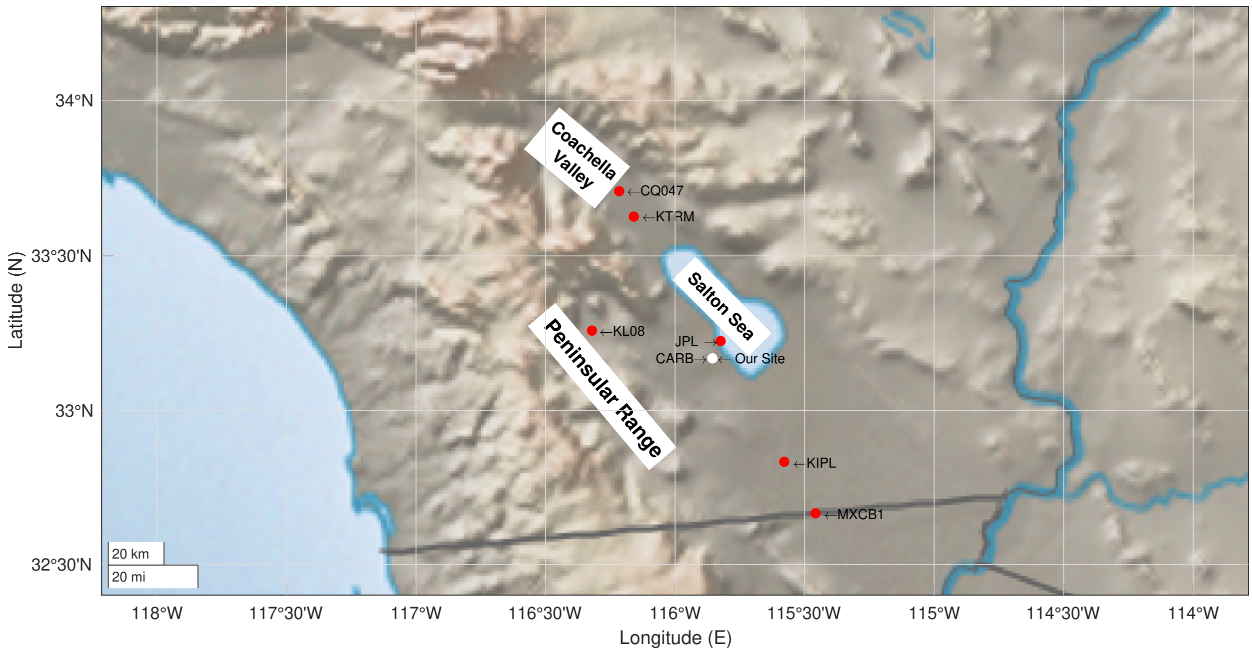

FIG. 1: Map of Salton Basin and surrounding topography in southeastern California. MESOWEST sites are the filled red cicles. The white circle indicates the location of our Salton Sea site and CARB site. The Peninsular Range lies to the west. To the north of the Sea is the Coachella Valley that terminates with a Transverse Range. To the south is a vast plain that gradually rises in elevation.

2020 as a case study. Next, I explain composite analyses of data over 2020 to illustrate the mode of background dust on background days. Finally, I discuss pathways for the transport of dust within the basin due to valley flows.

2. Data and methods

I utilize observations of coarse-mode and fine-mode Aerosol Optical Depth (AOD) from a CIMEL sun photometer from NASA's Aerosol Robotic Network (AERONET) (https://aeronet.gsfc.nasa.gov/). Aerosol optical depth estimates the amount of aerosols present by measuring the extinction of light due to aersols as light passes through our atmosphere. Coarse-mode AODs are mainly caused by larger particles (e.g., dust, sea-spray) while fine-mode AODs are smaller pollutants (e.g., soot, smoke). We utilize total AOD (coarse-mode + fine-mode AOD) because one AOD-mode may not completely represent all of the aerosols in that mode (i.e., some dust may be recognized as fine-mode AOD). This instrument is mounted on a new research station located within the Salton Basin managed by the Evan Research Lab. AOD measurements were utilized for 2020 through mid-May due to instrument error after this date. I also utilize PM_{10} measurements from a station maintained by the California Air Resources Board (CARB) (https://ww2.arb.ca.gov/). PM_{10} is particulate matter that is 10 microns or less in diameter. PM_{10} measurements were utilized in 2020 from late March to late May due to a lack of data prior in the beginning of the year.

Several surface meteorological stations positioned throughout the Salton Basin were utilized. These sites measure surface or near surface wind speed, wind direction and temperature, amongst others, and are maintained by the MESOWEST Network (https://mesowest.utah.edu/). Data is used from the beginning of 2020 up to early August.

I utilize LIDAR observations from a Vaisala Ceilometer CL51 during specific background dust days. Ceilometer data is used to analyze the position of aerosols and is a good proxy for analyzing the structure of the planetary boundary layer. Furthermore, upper-air observations were made using radiosondes attached to weather balloons during 29 February 2020. I utilize soundings created by these upper-air observations. Both of these data are provided by the Evan Research Lab (http://evan.ucsd.edu/Salton/). The locations of the sites utilized and topography are shown in Figure 1.

3. Results

a. 29 February 2020 case study

Firstly, we look at 29 February 2020. An upper-level low was situated over southern California leading to a weak synoptic forcing of westerly flow over the Salton Basin. Although this day is not fully representative of a background day, (i.e., a day in which dust emissions are

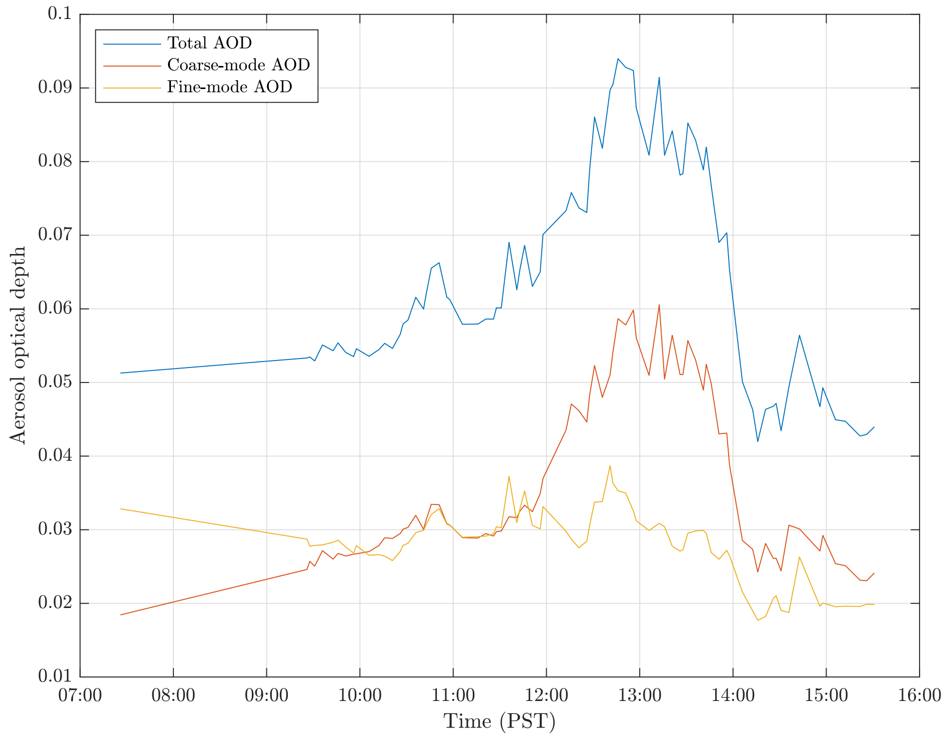

(a)

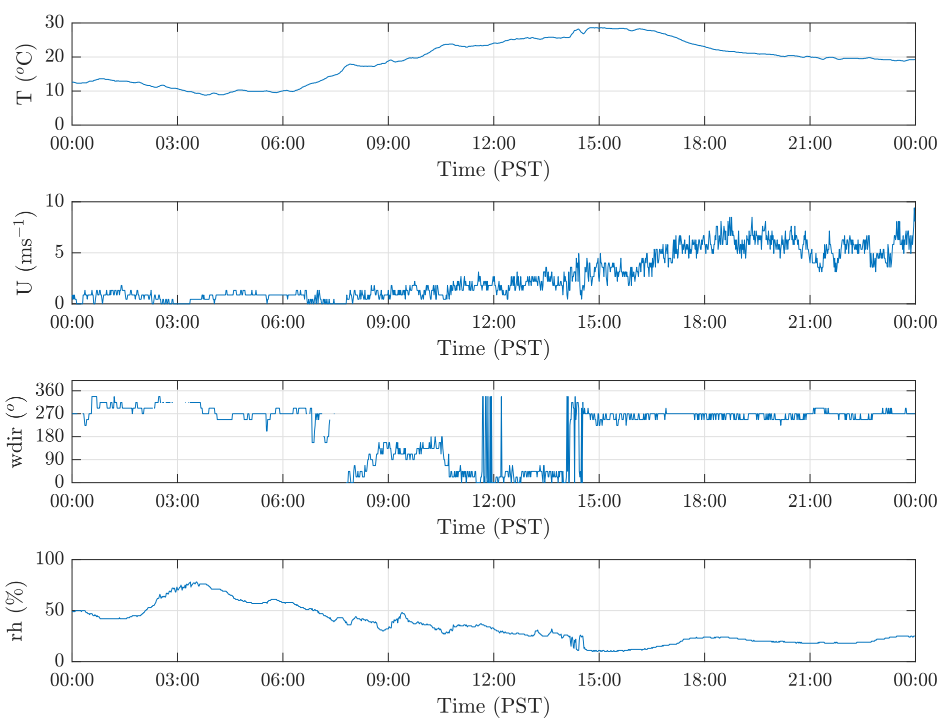

(b)

Fig. 2: (a) Aerosol optical depth observations on 29 February 2020 from an AERONET sun photometer. (b) Surface meteorological observations on 29 February 2020 from our Salton Sea met station. The parameters shown are temperature, wind speed, wind direction, and relative humidity, respectively. Parts of the wind direction data are missing around 0300 and 0700 PST. Both instruments located at our Salton Sea site indicated by the white dot in fig. 1.

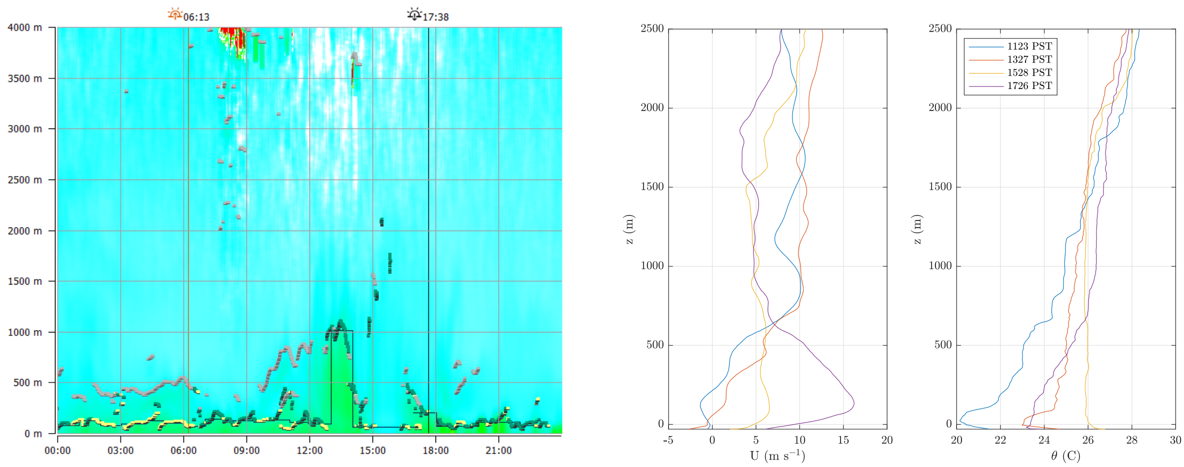

(a) (b)

Fig. 3: (a) Time series of ceilometer data on 29 February. Green squares represent aerosol concentrations. (b) Profiles of wind speed (left) and potential temperature (right) from weather balloons launched in the Salton Sea on 29 February 2020.

solely forced by convection and thermally-driven flows), we analyze conditions on this day because we have upper-air observations available. Here, I perform a detailed analysis discussing the forcing of dust.

From midnight to sunrise (0600 PST), conditions are calm indicated by surface meteorological conditions in fig. 2b. Temperatures are relatively low, hovering slightly above 10^{o}C and decrease throughout the night. Winds are out of the west at around 270^o and surprisingly weak in magnitude at near 1ms^{-1}. This could be the result of a strong nocturnal boundary layer (denser air) at the surface, not allowing the katabatic winds to increase wind speeds at the surface. In fig. 3a, we see a shallow layer of aerosols represented by the green and yellow squares. Their proximity to the surface suggests that the previous day's aerosols become trapped in the stable boundary layer forming at night.

At sunrise (0613 PST) to noon, the surface begins warming due to solar insolation. Wind speeds remain low throughout the remainder of the early morning, slowly starting to increase as we get closer to noon. At approximately 0700 PST, we see a shift in wind direction from westerly to easterly-southeasterly, suggesting the influence of anabatic flow due a pressure gradient caused by differential heating of the surrounding plain and nearby mountains. Ceilometer data depicts the layer of aerosols becoming slightly elevated indicating deepening of the mixed layer. Looking at fig. 2a, we observe a slow rise in total AOD from 0730 to 1030 PST and then a larger increase in total AOD until noon. A 1123 PST sounding in fig. 4 shows relatively large stable layer at the surface. In summary, weaker thermally-driven flows due to differential heating of topography initiate the gradual increase of dust concentrations in the atmosphere.

Table 1: Surface meteorological data on 29 February 2020 taken from MESOWEST site KL08 in the Anza Desert located approximately 50 km west of our Salton Sea Site. See fig. 1.

Time(PST)	Temperature (^oC)	Wind speed (m s^{-1})	Wind direction (^{o})
29-Feb-2020 10:55	25	4.6	240
29-Feb-2020 11:15	25	4.1	270
29-Feb-2020 11:35	25	3.1	280
29-Feb-2020 11:55	25	4.1	280
29-Feb-2020 12:15	25	5.7	250
29-Feb-2020 12:35	**25**	**7.2**	**260**
29-Feb-2020 12:55	27	6.2	260
29-Feb-2020 13:15	27	7.2	260
29-Feb-2020 13:35	**27**	**7.7**	**270**
29-Feb-2020 13:55	27	7.2	260
29-Feb-2020 14:15	27	6.1	260
29-Feb-2020 14:35	27	4.6	250

At noon, surface temperatures are notably higher near 25^{o}C and winds increase in magnitude, remaining steady around 2ms^{-1}. Interestingly, we see intermittent swings in surface wind direction from northeasterly to westerly depicted by the noisy signal at 1200 PST. This short-lived swing in wind direction out of the west suggests the arrival of high speed winds descending down the lee of the mountains to the west. Shown in table 1 are observations from a MESOWEST site in the Anza Desert, a relatively flat plain bordered by the steep slopes of the Peninsular Range. This site sees a significant increase in wind speeds due to the fast descending westerly flow. Concurrently, we see a significant increase in AOD at 1200 PST, peaking, and remaining at high levels until 1400 PST where AOD suddenly drops.

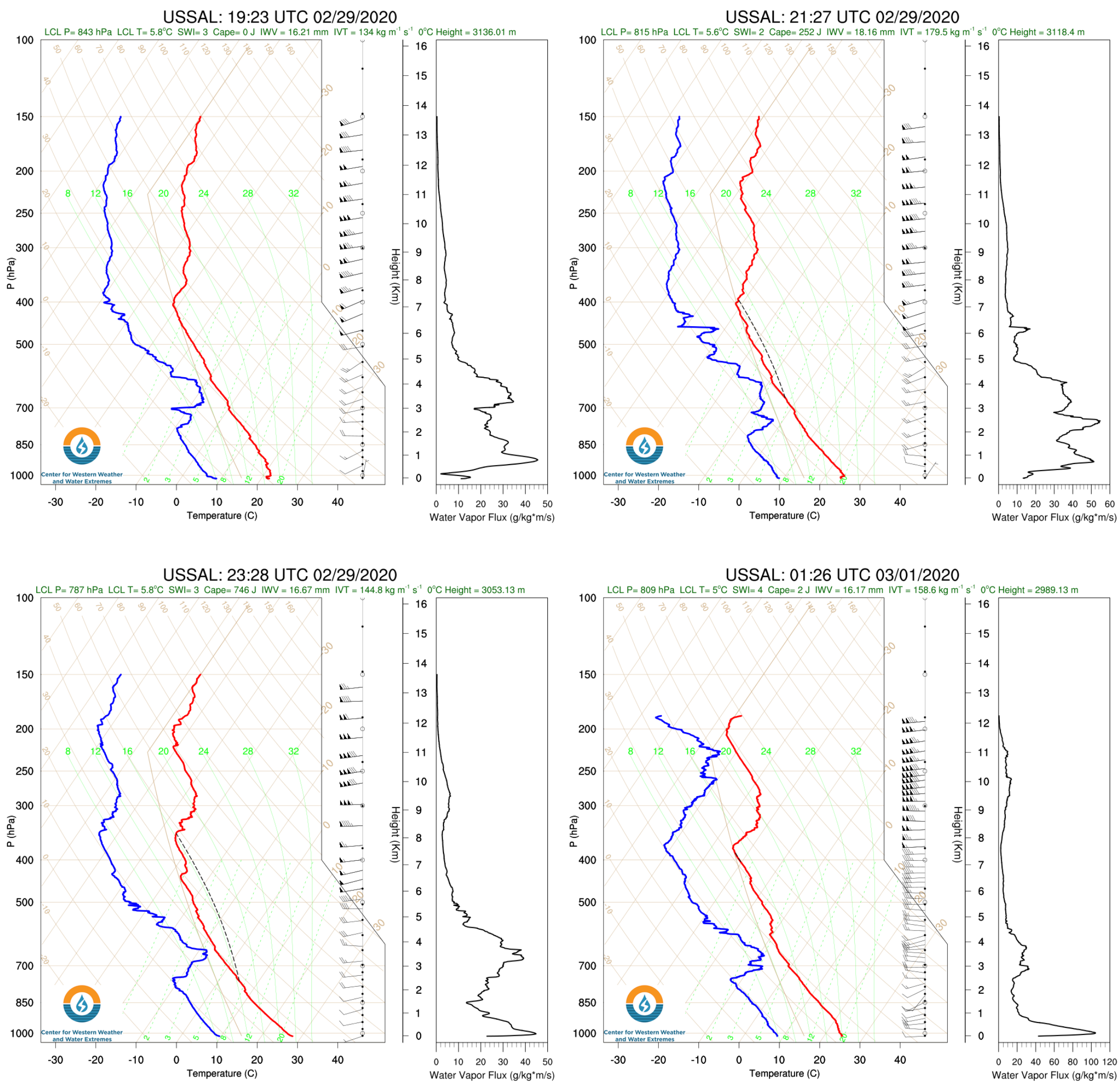

Fig. 4: Meteorological soundings from 29 February 2020. Time is specified in UTC (PST+8). Top left is 1123 PST, top right is 1327 PST, bottom left is 1528 PST, and bottom right is 1726 PST.

Moreover, ceilometer data during the same time interval shows aerosols elevated to 1km then drops rapidly at 1400 PST. The 1327 PST sounding still shows a small stable layer at the surface. A mixed layer, indicated by the isentropic temperature profile (constant potential temperature) extends from the top of the stable layer to around 1km. In total, data suggests that short bursts of high speed winds coming from the Anza Desert emit a cloud of dust which distributes throughout the mixed layer from 1230 - 1400 PST. This could explain the brief peaks in aerosol concentration and height at 1300 PST and abrupt decreases at 1400 PST, when the cloud of dust passes.

Looking at atmospheric wind speed profiles in fig. 3b, we observe in profile 2 (1327 PST) a strong westerly flow aloft. This represents the westerly flow of the free atmosphere. At 1400 PST, surface temperatures are approaching a maximum of 30^{o}C. Then, shown by the 1528 PST sounding, the stable layer has completely eroded and a well-defined mixed layer extends from the surface to approximately 2km. Interestingly, ceilometer data shows aerosols at heights of 1.5-2km but a clear lower atmosphere. Further exploration is required to explain this and for brevity, I will refrain from further discussion. Here, the mixed layer reaches a maximum and it is able to entrain westerly, free atmosphere

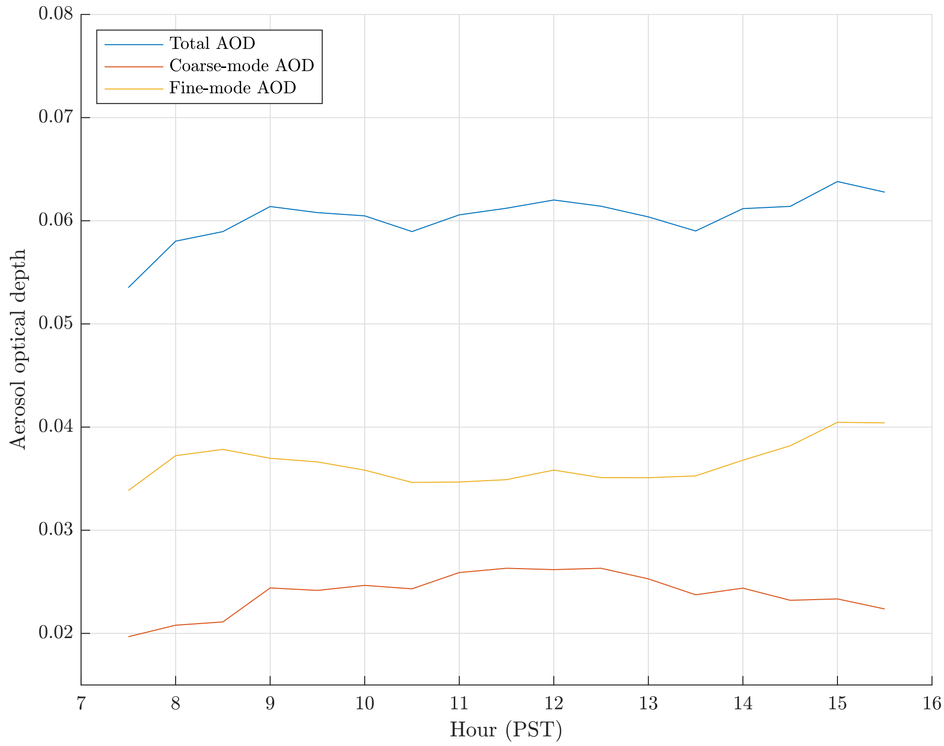

FIG. 5: Composite analysis of aerosol optical depth using data from the lowest 30% of basin wind speed days. Data is used from 1 January 2020 to 21 May 2020 due to data after being corrupted due to instrument error.

air downward into itself. Momentum is evenly distributed across the mixed layer indicated by profile 3 (1528 PST), where we see a decrease in upper level winds, a decrease in lower level winds, and ultimately a uniform, westerly wind speed profile (~5ms^{-1}) from the surface to around 2km height. Consequently, wind speeds increase at the surface, causing dust emission and dust distribution throughout the mixed layer, which we see in the ceilometer data. Note that we cannot use sun photometer data to observe dust in the atmosphere near sunset or sunrise due to the solar zenith angle being low, resulting in inaccurate AOD readings.

Close to sunset (1738 PST) temperatures decrease and the surface westerly winds increase in magnitude, suggesting the start of katabatic mountain flows. From the 1726 PST profiles in fig. 3b, we see that near-surface winds, a couple hundred meters above the surface, increase drastically more than surface winds. This suggests a nocturnal boundary layer already starting to form which we can almost observe in the sounding data. Lastly, we look at the ceilometer data. Throughout the night, concentrations of aerosols are shown to be confined in the stable boundary layer close to the surface. Sometimes we see aerosols become slightly elevated during the night which could be due to katabatic flows.

b. Composite Analysis of AOD

In order to capture days where dust emission is forced by background mechanisms (i.e., convection and thermally-driven flows) rather than high wind speed events (i.e., downslope windstorms), I perform a composite analysis using the bottom 30% of days with the lowest wind speeds. To get a good representative daily winds in the basin, I look at four different MESOWEST sites, CQ047, KTRM, KIPL and MXCB1 seen in fig. 1. First, I compute daily averages of wind speed for each site over each day in 2020 til early August. Then, for each day, I calculate an average wind speed for the entire basin by adding up the daily averages across the four sites. Finally, I take the bottom lowest 30% of windy days. By doing this, we can analyze data strictly representing *background days* where dust is forced purely by background mechanisms (i.e., convection and thermally-driven flows).

Next, I do a composite analysis of aerosol optical depth using data from only these background days as seen in fig. 5. Overall, we see total AOD slightly rise in the morning as a result of dry convection initiating. Then we see a slight peak in the afternoon at around 1500 PST, due to an increase in surface winds from the downward mixing of momentum when the mixed layer reaches a maximum. This shows that

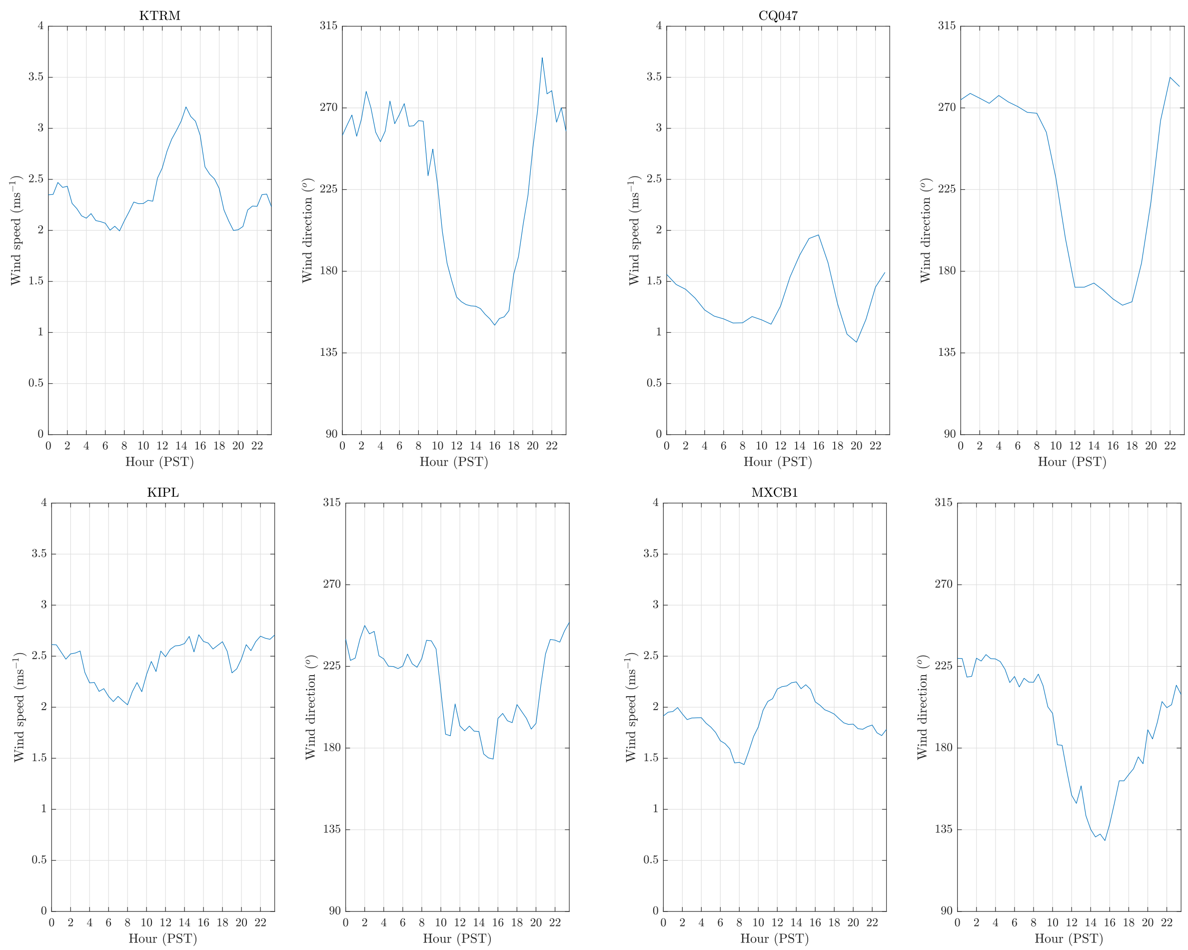

FIG. 6: Composite analysis of wind speed and wind direction from 4 different MESOWEST sites in the Salton Basin. I use data from the lowest 30% of basin wind speed days. KTRM, KIPL, and MXCB1 have high resolution data at 5 minute intervals. CQ047 has hourly data. I use data from the beginning of the year to early August. Wind directions are oriented as such: 0^o = northerly winds (coming from the north), 90^o = easterly winds, 180^o = southerly winds, 270^o = westerly winds.

there are moderate amounts of aerosols in the atmosphere even on days when wind speeds are low.

c. *Dust Transport: Valley Flows*

Next, I do a composite analysis of wind speeds and wind directions from several meteorological sites within the basin, looking only at background days. Thus, we can identify the pathways of background dust transport throughout the basin.

Sites KTRM and CQ047 are stationed in Coachella valley as seen in fig. 1. KTRM, which is further downvalley, is at an elevation of -38m. A moderate increase in elevation is observed going upvalley, noting CQ047 at an elevation of -8m. Mountains border the Coachella valley on all sides, however the western ranges are in closer proximity to the valley sites. It is important to note that the mountains to the west are oriented at an angle, such that the mountains are southwest of the sites. Sites KIPL and MXCB1 lie in the plains south of the Salton Sea where a gradual rise in elevation is observed southward. KIPL lies at -17m elevation and MXCB1, which is further south, lies at 4m above sea level. For reference, the Salton Sea is the lowest point of the basin at -72m elevation. Mountains lie to the west of the sites.

Now looking at the composite analyses for the two valley sites KTRM and CQ047 in fig. 6, we observe that the plots for wind speed and wind direction look fairly similar. Wind directions indicate a westerly flow during nighttime that shifts counter clockwise to southerly-southeasterly (SSE) at sunrise. SSE winds continue throughout the day until winds start to shift back to westerly at 1600 PST. We speculate the westerly flow during nighttime (and after sunset) is the resultant flow due to a NW downvalley flow and a SW katabatic flow. During the daytime, the plots indicate a SSE flow, which may be due to a SE upvalley flow and SW anabatic flow. KTRM observations confirm this however, CQ047 sees a much more southerly flow, which could be the result of a weaker SE valley flow due to CQ047 lying farther up the Coachella valley. Then, we see a shift back to westerly as daytime forcing shuts off and nighttime forcing turns on. Next, looking at the two plain sites in the southern part of the basin, we see that they also have similar shapes. Wind direction during nighttime is southwesterly (SW). They both shift counter clockwise however KIPL shifts towards southerly while MXCB1 shifts all the way to southeasterly (SE). The SW flow during the night may due to a westerly katabatic coupled with a southerly drainage flow. During the day, MXCB1 sees a net SE flow, which could be the result of a plain flow from MXCB1 to the smaller plain located at our Salton Sea site. We speculate a SE flow is generated due to the smaller plain warming faster than the larger plain south of the Sea, creating a thermal low west of the Sea and directing flow southeastward. The flows that add to a net SSE flow at KIPL are not obvious and further exploration is required to understand the pathway here.

These analyses suggest that dust from the southern plains and the Coachella valley are transported towards the Salton Sea via net drainage flows (a SSW drainage flow in the souther plains, and a net NW drainage flow in Coachella Valley). During the day, dust may be transported across the basin via a NW-SE plain-valley flow. By observing averaged wind directions at more sites, we can ideally identify background dust transport more thoroughly throughout the Salton Basin.

4. Conclusions

Here I analyzed conditions on 29 February 2020 to illustrate the mechanisms forcing dust. While this was not the ideal background day due to synoptic forcing, we analyze this day because we have upper-air observations available to understand the structure of the boundary layer. We observe a gradual rise in aerosol concentrations due to dry convection and a smaller rise later in the afternoon when surface winds increase due to a downward mixing of momentum. We also see that aerosol concentrations become elevated throughout the day as the mixed layer deepens. Future objectives include launching balloons on a true background dust day in order to observe how the mixed layer deepens and where aerosol concentrations are dispersed without the forcing of synoptic systems. Next, we performed an analysis over all the lowest 30% of basin wind speed days (i.e., looking at background forced days). We find a consistent, moderate concentration of dust that slowly increases with in the morning and then somewhat peaks in the afternoon when the mixed layer deepens fully and surface winds increase. Next steps include doing a composite analysis ceilometer data on these background days. Lastly, we did a composite analysis of wind speed and wind direction over 4 sites across the Salton Basin. We find that a net drainage flow towards the Salton Sea during the night and a daytime NW-SE across basin flow that could represent pathways of dust. Next steps here would be to identify valid surface meteorological stations located in other parts of the basin (e.g., east and west) and analyze data from these stations. Furthermore, we could identify an area where data may be crucial but lacking and set up a meteorological station to understand dust transport.

Acknowledgments. The author thanks Amato Evan and Trinity Robinson for their guidance on this project. Further acknowledgements to the Hiestand Undergraduate Research Scholarship for funding this work.

Data availability statement. Data are publicly provided by the MesoWest network (https://mesowest.utah.edu/), California Air Resources Board (https://ww2.arb.ca.gov/), and NASA (https://aeronet.gsfc.nasa.gov/). Selective data is publicly provided by the Evan Research Lab (http://evan.ucsd.edu/Salton/). Datasets and MatLab scripts used in analysis can be found here (https://github.com/tbarbero/Summer_2020).

References

, 2010a: *The Boundary Layer*, chap. 4, 73–114. John Wiley Sons, Ltd, doi:10.1002/9780470682104.ch4, URL https://onlinelibrary.wiley.com/doi/abs/10.1002/9780470682104.ch4, https://onlinelibrary.wiley.com/doi/pdf/10.1002/9780470682104.ch4.

, 2010b: *Mountain Waves and Downslope Windstorms*, chap. 12, 327–342. John Wiley Sons, Ltd, doi:10.1002/9780470682104.ch12, URL https://onlinelibrary.wiley.com/doi/abs/10.1002/9780470682104.ch12, https://onlinelibrary.wiley.com/doi/pdf/10.1002/9780470682104.ch12.

, 2010c: *Thermally Forced Winds in Mountainous Terrain*, chap. 11, 317–325. John Wiley Sons, Ltd, doi:10.1002/9780470682104.ch11, URL https://onlinelibrary.wiley.com/doi/abs/10.1002/9780470682104.ch11, https://onlinelibrary.wiley.com/doi/pdf/10.1002/9780470682104.ch11.

Evan, A., 2019: Downslope winds and dust storms in the salton basin. *Monthly Weather Review*, **147**, doi:10.1175/MWR-D-18-0357.1.

Forsman, T. N., 2014: What the qsa means for the salton sea: California's big blank check. *Ariz. St. LJ*, **46**, 365.

Ives, R. L., 1949: Climate of the sonoran desert region. *Annals of the Association of American Geographers*, **39 (3)**, 143–187, doi:10.1080/00045604909352003.